# Temperature dependence of lattice dynamics of lithium 7

M. M. Beg* and M. Nielsen
*Danish Atomic Energy Commission Research Establishment Risø, DK-4000 Roskilde, Denmark*
(Received 22 September 1975; revised manuscript received 7 July 1976)

Phonon dispersion relations in $^7$Li have been measured by the coherent inelastic neutron scattering at 293 and 110 K. The frequency distributions are obtained from the experimental data using the Born–von Kármán general force model. The first-neighbor force constants at 293 K are found to be about 10% smaller than those at 100 K. Temperature dependences of selected phonons have been studied from 110 K to near the melting point. The energy shifts and phonon linewidths have been evaluated at 293, 383, and 424 K by comparing the widths and energies to those measured at 110 K. The lattice parameter is found to be $3.490 \pm 0.003$ Å at 110 K and $3.537 \pm 0.003$ Å at 424 K. The elastic constants obtained at 293 K from the model parameters are ($10^{11}$ dyn/cm$^2$) $C_{11} = 1.73 \pm 0.10$, $C_{12} = 1.31 \pm 0.20$, and $C_{44} = 0.84 \pm 0.060$. The temperature dependence of elastic constants is also determined.

## I. INTRODUCTION

Measurement of phonon dispersion relations of lithium have been made[1] at 98 K, and an analysis of the data applying a Born–von Kármán force model shows that the interatomic forces up to five or six neighbors are important. Some calculations on the pseudopotential model[2] have also been reported which predict correctly the crossover of the $[\zeta 00]$L and $[\zeta 00]$T branches.

In the neutron scattering experiments on the alkali metals lithium,[1] sodium,[3,4] and rubidium[5] a number of extra peaks have been observed, especially in the $[\zeta 00]$L symmetry direction. For sodium[4] the phonons observed in the $[\zeta\zeta\zeta]$T direction have been found to be unexpectedly broad and sometimes split into two peaks. Cowley and Pant[6] have shown that this can be explained by the relaxed vertical momentum resolution of the spectrometer. Smith *et al.*[7] did not include the $[\zeta\zeta\zeta]$T phonons below $\zeta = 0.5$ in their calculations of the force constants for lithium.

In the present work the phonon dispersion relations at 293 K have been measured in detail and the results have been analyzed using the five-neighbor Born–von Kármán general force model. Measurements for the $[\zeta\zeta\zeta]$T branch at liquid-nitrogen temperature have been performed again and the present data have been added to the data of Smith *et al.*[1] to recalculate the force constants. Detailed resolution calculations involving the phonon eigenvectors have been performed to explain the satellites in the $[00\zeta]$L branch and the broad groups in the $[\zeta\zeta\zeta]$T branch. The temperature dependence of selected phonons has been studied for temperatures from 110 to 424 K. The values for the lattice constant for $^7$Li, the elastic constants, the variation in phonon energies, and the phonon linewidths have been obtained at temperatures up to near the melting point.

## II. EXPERIMENTAL SPECIFICATIONS

The coherent inelastic neutron scattering from single crystals of $^7$Li was studied using a triple-axis spectrometer at the DR3 reactor at Risø. Pyrolytic graphite crystals were used as monochromator and analyzer. The spectrometer was operated in the constant-$Q$ mode and all the measurements were made for the neutron-energy-loss process. Variable incident energy was used during all the phonon scans and the analyzer energy was kept constant at 14.5 meV. A 5-cm-thick graphite filter was placed in the scattered beam to suppress the second-order Bragg scattering from the analyzer crystal.

The single crystals of $^7$Li were grown by the Bridgman method, with the lithium metal sealed in specially designed thin-walled (0.5 mm) stainless-steel containers.[8] Four crystals were used during the present measurements. They were 6 cm long; crystals 1 and 3 had a diameter of 1.1 cm, whereas crystals 2 and 4 had a diameter of 2.2 cm. The mosaic spread of the crystals ranged between 0.3° and 1.5°. Crystals 1, 3, and 4 had the [110] direction almost parallel to the axes of the container, while crystal 2 had the [100] direction parallel to that axis. Most of the measurements were made on crystals 2 and 4. However, the smaller-diameter crystals were used to check some of the measurements from the thicker crystals, and no systematic error was found due to the sample thickness. All the temperature-dependent observations were taken with crystal 4 set with its $(1\bar{1}0)$ plane parallel to the scattering plane. This crystal had a mosaic spread of 0.48°. The crystal had another small grain with a Bragg intensity about 100 times less than that from the main crystal. This grain did not affect the phonon scans much, although in some scans the grain contributed small humps on the wings of the phonon peaks.

TABLE I. Phonon energies (meV) obtained by coherent inelastic neutron scattering along three symmetry directions [ζ00], [ζζ0], and [ζζζ] in $^7$Li at 293 K.

| $\zeta = aq/2\pi$ | $\omega$ | $\zeta = (1/\sqrt{2})(aq/2\pi)$ | $\omega$ | $\zeta = (1/\sqrt{3})(aq/2\pi)$ | $\omega$ |
|---|---|---|---|---|---|
| [100] L | | [110] L | | [111] L | |
| 0.112 | 7.6 ± 0.3 | 0.04 | 4.5 ± 0.3 | 0.097 | 13.0 ± 1.0 |
| 0.168 | 10.9 ± 0.5 | 0.08 | 8.6 ± 0.3 | 0.161 | 20.8 ± 1.0 |
| 0.196 | 12.3 ± 0.5 | 0.119 | 12.8 ± 0.6 | 0.226 | 27.5 ± 0.6 |
| 0.223 | 14.2 ± 0.5 | 0.158 | 16.8 ± 0.6 | 0.290 | 31.8 ± 1.0 |
| 0.279 | 17.0 ± 0.5 | 0.237 | 24.8 ± 0.6 | 0.355 | 33.3 ± 1.2 |
| 0.335 | 19.9 ± 0.5 | 0.316 | 30.8 ± 0.6 | 0.451 | 30.3 ± 0.8 |
| 0.363 | 20.5 ± 0.5 | 0.356 | 33.0 ± 0.5 | 0.548 | 25.2 ± 0.8 |
| 0.447 | 25.1 ± 1.0 | 0.375 | 34.0 ± 0.5 | 0.645 | 16.5 ± 0.6 |
| 0.503 | 27.5 ± 1.0 | 0.395 | 34.5 ± 0.5 | 0.677 | 15.0 ± 0.5 |
| 0.559 | 27.1 ± 1.0 | 0.435 | 35.8 ± 0.6 | 0.710 | 14.2 ± 1.0 |
| 0.614 | 28.0 ± 0.7 | 0.50 | 36.5 ± 0.5 | 0.742 | 17.0 ± 0.8 |
| 0.670 | 30.0 ± 0.8 | | | 0.839 | 27.3 ± 1.0 |
| 0.782 | 32.2 ± 0.8 | [110] $T_1$ | | 1.00 | 36.0 ± 1.0 |
| 0.950 | 35.6 ± 0.6 | 0.08 | 2.2 ± 0.3 | | |
| 1.00 | 36.0 ± 1.0 | 0.138 | 3.7 ± 0.3 | [111] T | |
| | | 0.198 | 4.9 ± 0.4 | 0.097 | 6.4 ± 0.5 |
| [100] T | | 0.257 | 6.0 ± 0.5 | 0.129 | 8.4 ± 0.5 |
| 0.112 | 5.1 ± 0.3 | 0.316 | 7.2 ± 0.5 | 0.161 | 9.0 ± 0.5 |
| 0.168 | 7.9 ± 0.4 | 0.356 | 7.3 ± 0.6 | 0.194 | 11.7 ± 0.6 |
| 0.223 | 10.6 ± 0.4 | 0.407 | 8.0 ± 0.6 | 0.226 | 12.7 ± 0.6 |
| 0.279 | 13.2 ± 0.5 | 0.50 | 8.6 ± 0.6 | 0.258 | 15.2 ± 0.6 |
| 0.335 | 16.5 ± 0.6 | | | 0.290 | 18.3 ± 0.8 |
| 0.391 | 20.0 ± 0.8 | [110] $T_2$ | | 0.323 | 20.0 ± 1.0 |
| 0.447 | 23.1 ± 1.0 | 0.08 | 5.0 ± 0.3 | 0.355 | 23.5 ± 1.2 |
| 0.559 | 27.5 ± 0.6 | 0.119 | 7.5 ± 0.4 | 0.419 | 26.0 ± 1.0 |
| 0.614 | 29.7 ± 0.6 | 0.158 | 10.3 ± 0.5 | 0.451 | 27.7 ± 0.8 |
| 0.782 | 33.3 ± 1.0 | 0.198 | 13.0 ± 0.5 | 0.548 | 29.3 ± 0.8 |
| 1.00 | 36.0 ± 1.0 | 0.237 | 14.8 ± 0.5 | 0.710 | 33.5 ± 0.6 |
| | | 0.316 | 18.1 ± 0.5 | 0.774 | 34.0 ± 0.8 |
| | | 0.356 | 19.6 ± 0.5 | 1.00 | 36.0 ± 1.0 |
| | | 0.435 | 21.5 ± 0.5 | | |
| | | 0.50 | 22.2 ± 0.5 | | |

These humps disappeared or changed their intensities by redefining the slits in the incident and the scattered beams. Any humps due to the small grains were easily recognizable as separate from the extra peaks occurring owing to the relaxed resolution effects. A curved graphite monochromator was used, which focused in the incident beam on to about 3 cm height of the sample. Some of the peaks due to the grains could be removed by focusing the beam on a better part of the crystal. No such manipulation was needed for crystal 2. The slits used to define the beam for the 2.2-cm-thick crystals had dimensions $3 \times 1.5$ cm$^2$. The slits were chose narrower than the crystal thickness to reduce the scattering from the container walls.

All the collimators and the slits were kept constant throughout the temperature-dependent measurements. The temperatures were recorded by a platinum resistance thermometer embedded near the crystal base in the liquid-nitrogen cryostat. The same cryostat could be heated to 424 K, so that the measurement was made without a need to reset the crystal for the low-temperature and the high-temperature runs separately.

In all more than 200 phonon scans were made, mostly at room temperature. Sixty scans for selected phonons were performed at four temperatures, from 110 to 424 K. The highest temperature reached was 0.94 of the melting point of lithium. During a scan the temperature remained constant within ± 1 K.

## III. RESULTS AND DISCUSSION

### A. Frequency distribution

Phonon dispersion relations were measured at 293 K along the [ζ00], [ζζ0], and [ζζζ] directions and Table I gives the frequencies. The data have been analyzed on the basis of a five-neighbor Born–von Kármán general force model. Figure 1 shows the observed points and the fitted curves in the three symmetry directions. The fifth-neighbor constants are found to be about 3% of the first-

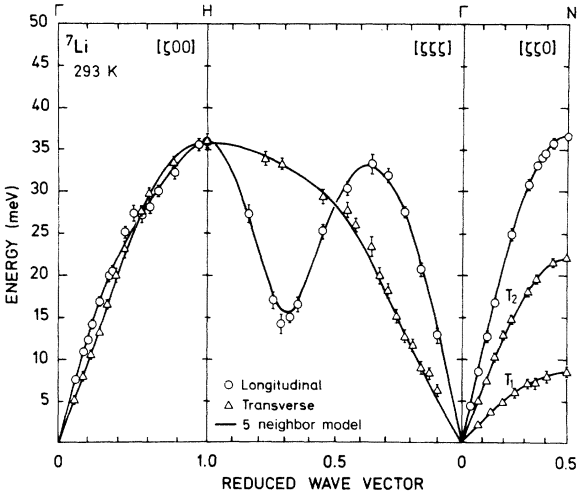


FIG. 1. Phonon dispersion relations at 293 K in the three symmetry directions [ζ00], [ζζ0], and [ζζζ]. ○ and Δ represent the longitudinal and transverse acoustic modes, respectively. The solid lines are five-neighbor Born–von Kármán general model fit. All the wave vectors are in reduced coordinates.

neighbor force constants, and their magnitude is of the same order as the standard errors on the force constants. Therefore, a five-neighbor Born–von Kármán fit is considered adequate to the room-temperature data. Smith *et al.*,[1] in their analysis of the 98-K measurements, find it necessary to include the forces at least to six neighbors. The force constants at 293 K are compared with the 98-K results in Table II. At room temperature the first-neighbor forces are about 10% smaller than those at the lower temperature.

The dispersion curves exhibit the crossover of [ζ00]L and [ζ00]T branches as observed at 98 K in Li,[1] and at 90 K for sodium.[3] But after the crossover the energy gap between the two branches is less at 293 K than at 98 K. Smith *et al.*[7] observed two unequal split peaks for phonons in the [ζζζ]T branch for $\zeta < 0.5$, and they did not use that data in their analysis. As observed by many authors,[4–9] broad or split phonons are observed in anisotropic cubic materials in the [ζζζ]T branch, and the effect persists up to the zone boundary. The phonons can split into two peaks as discussed by Cowley and Pant[6] and the effect depends on the spectrometer resolution. We have observed split, broad, and double-peaked phonon groups in $^7$Li in the [ζζζ]T direction, but they were evenly balanced around the central position and their energies could be evaluated. Some of the phonon groups for [ζζζ]T branch at 110 K for different ζ vectors are shown in Fig. 2. As shown in Fig. 3 the model calculations by Smith *et al.*[1] for the [ζζζ]T branch

TABLE II. Force constants (units dyn/cm) calculated on the Born–von Kármán general force model. The values obtained for a five-neighbor fit at 293 K are given in column I. In column II are the values obtained by Smith *et al.* (Ref. 1) at 98 K. Column III gives the five-neighbor force constants at low temperature, with the present data for the [ζζζ] T branch at 110 K combined with the previous measurements (Ref. 1).

| $n$ | | 293-K five neighbor I | 98-K six neighbor (Ref. 1) II | 98 K (Ref. 1) plus present work 110-K five-neighbor III |
|---|---|---|---|---|
| 1 | $\alpha_1$ | 2114 ± 33 | 2336 ± 29 | 2271 ± 127 |
| | $\beta_1$ | 2207 ± 35 | 2462 ± 38 | 2360 ± 182 |
| 2 | $\alpha_2$ | 862 ± 79 | 694 ± 66 | 790 ± 376 |
| | $\beta_2$ | 16 ± 54 | 140 ± 46 | 163 ± 301 |
| 3 | $\alpha_3$ | −268 ± 28 | −277 ± 26 | −368 ± 148 |
| | $\beta_3$ | 55 ± 40 | 125 ± 34 | 58 ± 191 |
| | $\gamma_3$ | −197 ± 76 | −158 ± 38 | −657 ± 392 |
| 4 | $\alpha_4$ | 146 ± 24 | 171 ± 26 | 180 ± 41 |
| | $\beta_4$ | −57 ± 12 | −126 ± 17 | −71 ± 62 |
| | $\gamma_4$ | 33 ± 30 | −122 ± 34 | 64 ± 154 |
| | $\delta_4$ | 52 ± 21 | 11 ± 26 | 79 ± 110 |
| 5 | $\alpha_5$ | 62 ± 19 | 148 ± 17 | 112 ± 98 |
| | $\beta_5$ | −0.77 ± 47 | −38 ± 41 | 184 ± 220 |
| 6 | $\alpha_6$ | | −282 ± 60 | |
| | $\beta_6$ | | 12 ± 36 | |

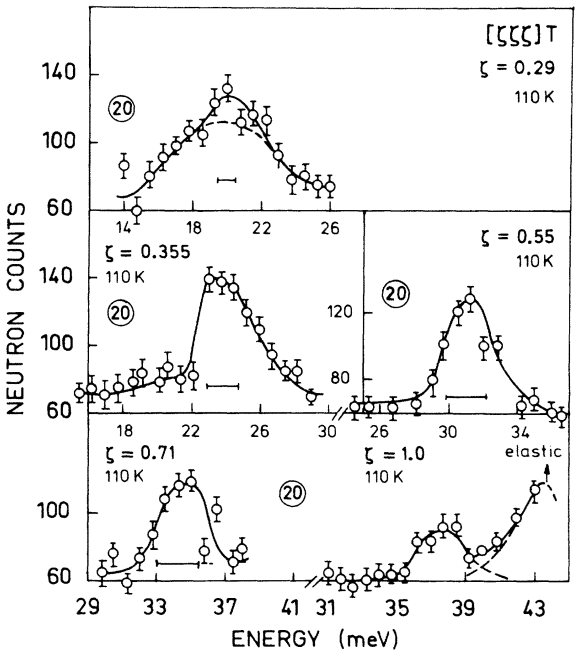


FIG. 2. Some of the broad phonon groups observed for the [ζζζ]T branch in $^7$Li at 110 K. The rise in intensity at the higher-energy end of the zone-boundary phonon ($\zeta = 1$) is due to the higher-order elastic contamination which peaks at 43.5 meV. The numbers in circles are the monitor counts for which measurements were made.

show a large discrepancy with the present measurements for $\zeta < 0.5$. The Born–von Kármán general model calculations were performed after combining the present data at 110 K with the 98-K data of Smith *et al.*[1] and the force constants at low temperature were recalculated. The new force constants are given in column III of Table II.

The force constants given in Table II were used to calculate the frequency distribution at 293 K, using the extrapolation method of Gilat and Raubenheimer.[10] As a check we calculated the frequency distribution for lithium using the six-neighbor force constants of Smith *et al.*[1] and we reproduced their distribution. The frequency distributions at 293 and 98 K are compared in Fig. 4. The main difference between the two functions is that the peak around $8.8 \times 10^{12}$ Hz, marked $E$ in Fig. 4, is no longer split at 293 K, but is a broader peak of lower intensity.

The frequency distribution at 293 K was used to calculate the Debye temperature $\Theta_D$. The results

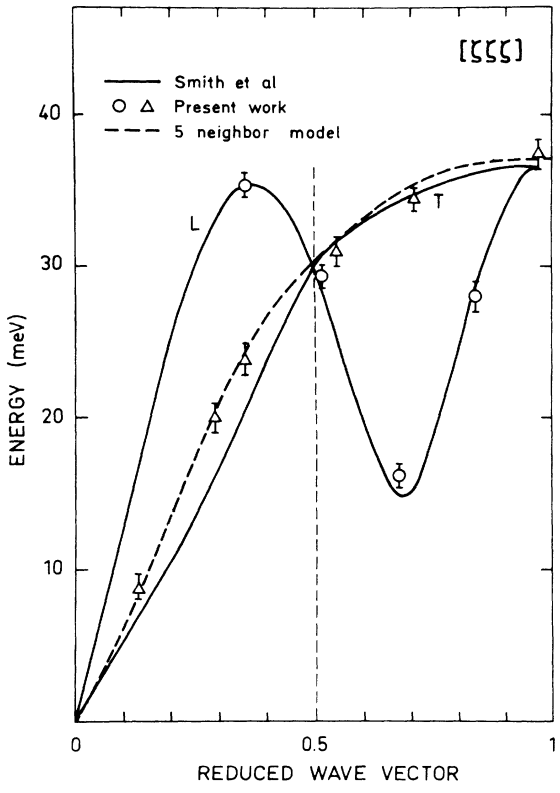


FIG. 3. Observed phonon energies for the [ζζζ]T branch at 100 K are compared with the model calculations tions of Smith *et al.* (Ref. 1) (solid lines). The present observations give considerably higher phonon energies for this branch than the previous model calculations. Dashed line shows the recalculated five-neighbor Born–von Kármán model fit with the combined data of the two works.

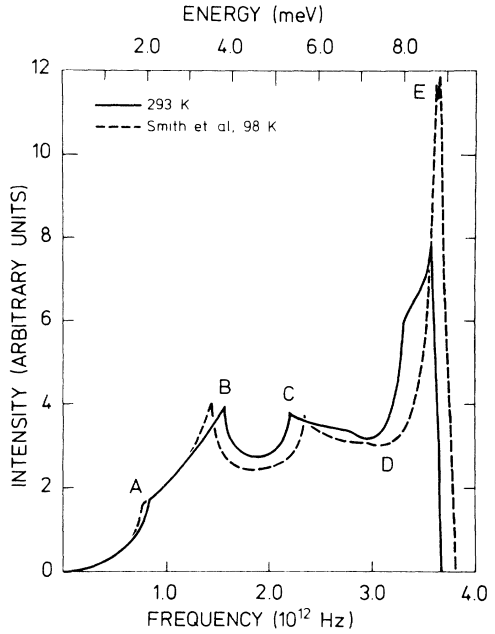


FIG. 4. Comparison of frequency distributions in $^7$Li at two temperatures. Solid line: 293 K, present work; dashed line: 98 K, Smith *et al.* (Ref. 1).

are compared with the specific-heat measurements[11] in Fig. 5. The $\Theta_D$'s obtained by Smith *et al.*[1] are also plotted. The specific-heat data are influenced by the phase transition at 78 K at low temperatures. At high temperatures the anharmonic effects are important and they affect the specific-heat $\Theta_D$ much stronger than $\Theta_D$ determined by neutron scattering.[12]

### B. Temperature dependence of lattice parameter and the elastic constants

The lattice parameter for $^7$Li was determined at five temperatures ranging from 110 to 424 K. The values are given in Table III and they are compared with the result of x-ray measurements[13,14] in Fig. 6.

The elastic constants were obtained from the low-energy phonons measured in the three symmetry directions. The constants at 293 K were calculated using the force constants obtained by the five-neighbor Born–von Kármán model. The elastic constants at various temperatures are listed in Table III. The volume dependence of the elastic constants is shown in Fig. 7. The values of the elastic constants obtained by Nash and Smith[15] and Jain[16] from the sound-echo technique are also plotted. The elastic constants obtained by the present measurements are up to 20% higher than the sound-echo measurements. The shear constant $C_{44}$ varies much faster with the change in volume than $C_{11}$ does.

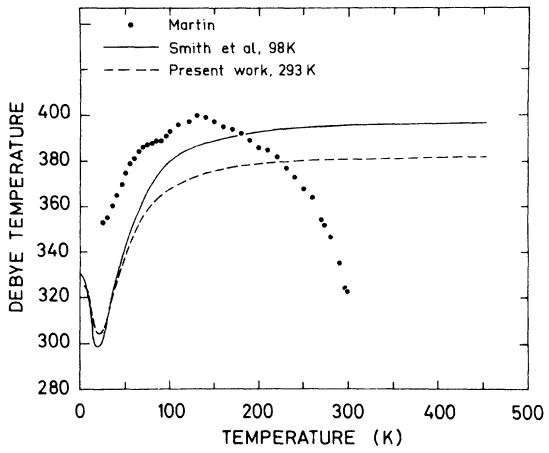


FIG. 5. Debye $\Theta_D$ vs temperature. Solid line gives the values evaluated from neutron data at 98 K (Ref. 1) on the harmonic approximation. Dotted line shows the values calculated from the present data at 293 K. Solid circles are the values obtained from the specific-heat measurements (Ref. 11).

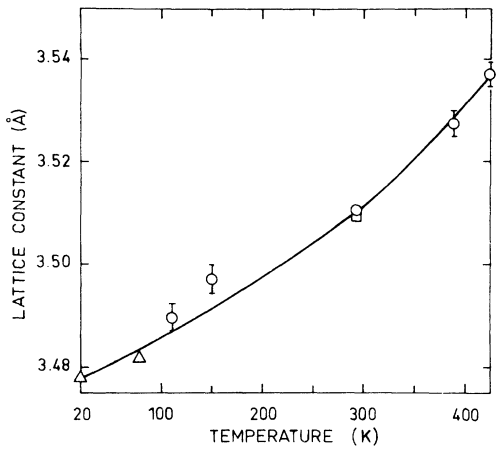


FIG. 6. Temperature dependence of lattice parameter of $^7$Li. ○: present measurements, Δ: x ray (Ref. 13) at 20 and 78 K, □: x ray at 293 K. The error bars include the error on the wavelength measurements.

### C. Temperature dependence of phonons

Selected phonon groups were studied as functions of temperature from 110 to 424 K, which is 0.94 times the melting temperature. Some of the groups for the $[\zeta\zeta 0]$T and $[\zeta\zeta\zeta]$L phonon branches are shown in Figs. 8 and 9.

Each neutron group was measured at different temperatures at the same point in the reciprocal space and with the same resolution. The width and the energy shifts of the phonons were evaluated by comparison with the groups measured at 110 K. In this procedure it was assumed that the linewidths were negligible at 110 K. Some of the groups, especially at high temperatures, had a sloping background, and this was extrapolated linearly between the two wings of the groups and subtracted. The frequency of each mode was taken to be the center position of the corrected group. The observed full width at half-maximum was taken to be equal to the root-mean-square sum of the resolution and phonon widths. Final values for the phonon energies and line widths are given in Table IV. The linewidths for some of the phonons could not be evaluated owing to interference from another phonon branch and in a few cases owing to the wings not being properly defined. The uncertainty on the linewidths are evaluated from the sum of squares of the individual uncertainties, and do not contain errors due to the Gaussian approximation for the phonon line shapes. The temperature variations of the phonon energy and width are found to depend on the momentum vector ($\vec{q}$) and this is shown in Fig. 10. The phonons near the zone boundary show energy shifts of (10–12)%. The $[\zeta\zeta\zeta]$L $\zeta = 0.677$ phonon shown in Fig. 9, which lies on the dip in the [111]L branch, shows about 20% shift in energy near the melting point. The phonon at the zone

TABLE III. Elastic constants (units $10^{11}$ dyn/cm$^2$) and the lattice parameter $a$ for $^7$Li at different temperatures. Errors on $a$ include the errors in the neutron wavelength measurements.

| Temperature (K) | $C_{11}$ | $C_{44}$ | $C_{12}$ | $a$ (Å) |
|---|---|---|---|---|
| 110 | 1.77 ± 0.14 | 1.08 ± 0.10 | 1.32 ± 0.25 | 3.490 ± 0.003 |
| 150 | | | | 3.497 ± 0.003 |
| 293 | 1.73 ± 0.10 | 0.84 ± 0.06 | 1.31 ± 0.20 | 3.5105 ± 0.0010 |
| 385 | 1.71 ± 0.14 | 0.73 ± 0.08 | 1.14 ± 0.25 | 3.528 ± 0.003 |
| 424 | 1.62 ± 0.15 | 0.74 ± 0.08 | 1.19 ± 0.25 | 3.537 ± 0.003 |

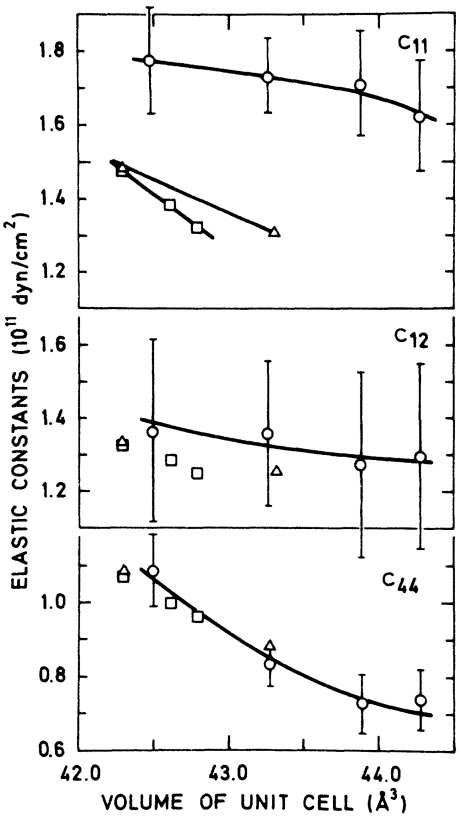


FIG. 7. Volume dependence of the elastic constant. The values of the elastic constants obtained by the sound-echo technique are also shown. ○: present measurements; □: Nash and Smith (Ref. 15); △: Jain (Ref. 16). The measurements at the largest volume correspond to a temperature of 0.94 of the melting point. The lines are guides to the eye.

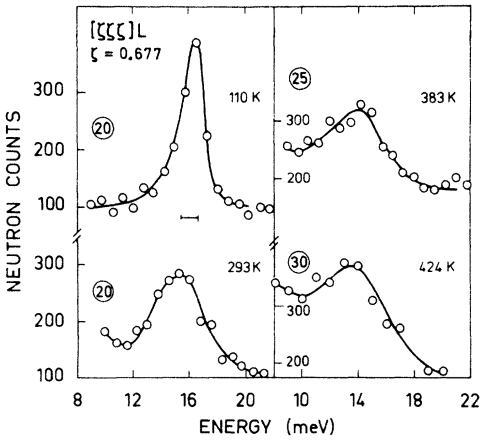


FIG. 9. Temperature dependence of the [ζζζ]L group measured at $(2-\zeta, 2-\zeta, 2-\zeta)$ with $\zeta = 0.677$. The figures in circles are the monitor counts for which measurements were made. The horizontal bars represent the instrumental resolution in the planar approximation.

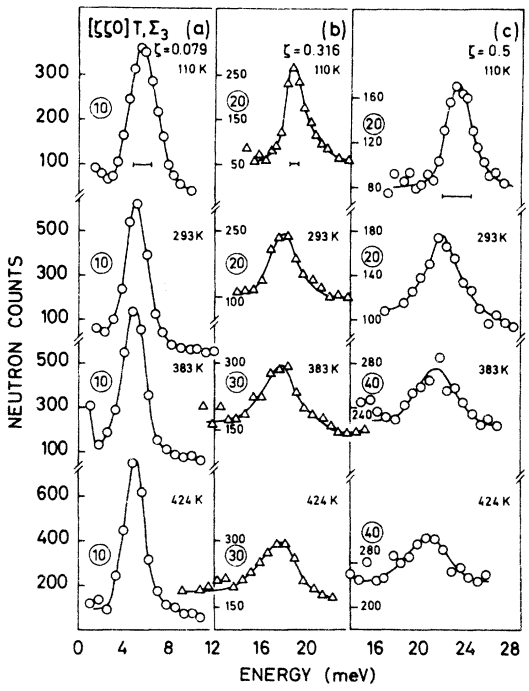


FIG. 8. Phonon groups for $[\zeta\zeta 0]T_2$, $\Sigma_3$ branch measured at $(-\zeta, -\zeta, 2)$. (a) $\zeta = 0.079$, (b) $\zeta = 0.316$, and (c) $\zeta = 0.5$ the zone boundary. The horizontal bars show the resolution width calculated in the planar approximation. The figures in circles are the monitor counts for which measurements were made. The temperatures are given in the figure.

boundary $H$ was measured at the reciprocal-lattice point $\bar{1}\bar{1}\bar{1}$. The phonons measured near these points showed some splitting due to the resolution effects. If the shape of the dispersion surface in that region is temperature dependent the widths

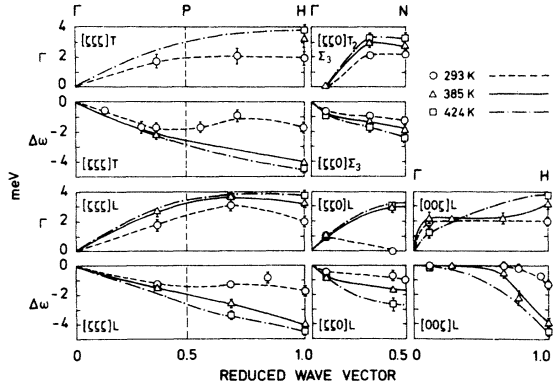


FIG. 10. Phonon energy shifts and half-widths in $^7$Li at three temperatures: ○–293 K, △–383 K, □–424 K. Lines are guides to the eye.

TABLE IV. Measured widths and energies (units meV) for phonons observed in the three symmetry directions $[\zeta 00]$, $[\zeta\zeta 0]$, and $[\zeta\zeta\zeta]$ in lithium. $\omega$ is the energy of phonon, $W$ is the observed width, $T$ is the temperature in K, and $\Gamma$ is the phonon linewidth (meV) evaluated by comparison of the observed width at $T$ with that observed at 110 K.

| $\zeta$ | $\omega$ | $W$ | $T$ | $\Gamma$ | $\zeta$ | $\omega$ | $W$ | $T$ | $\Gamma$ |
|---|---|---|---|---|---|---|---|---|---|
| | | $[00\zeta]$ L | | | | | $[\zeta\zeta 0]$ L | | |
| 0.112 | 7.6 ± 0.2 | 2.0 ± 0.2 | 112 | | 0.079 | 9.0 ± 0.2 | 1.5 ± 0.1 | 143 | |
| | 7.6 ± 0.2 | 2.8 ± 0.3 | 293 | 1.96 ± 0.36 | | 8.6 ± 0.2 | 1.9 ± 0.1 | 293 | 1.17 ± 0.15 |
| | 7.6 ± 0.2 | 3.0 ± 0.3 | 383 | 2.24 ± 0.36 | | 8.2 ± 0.2 | 1.9 ± 0.1 | 397 | 1.17 ± 0.15 |
| | 7.4 ± 0.2 | 2.4 ± 0.5 | 424 | 1.33 ± 0.54 | | 8.2 ± 0.2 | 1.8 ± 0.1 | | 1.00 ± 0.15 |
| 0.28 | 17.0 ± 0.3 | 2.3 ± 0.2 | 138 | | 0.435 | 37.2 ± 0.5 | 1.8 ± 0.2 | 143 | |
| | 17.0 ± 0.3 | | 293 | | | 36.5 ± 0.5 | 1.8 ± 0.2 | 293 | 0.0 ± 0.3 |
| | 17.0 ± 0.3 | 3.2 ± 0.3 | 383 | 2.22 ± 0.36 | | 35.6 ± 0.5 | 3.5 ± 0.4 | 395 | 3.0 ± 0.45 |
| 0.67 | 30.0 ± 0.5 | 2.0 ± 0.2 | 114 | | | 35.1 ± 0.5 | 3.6 ± 0.4 | 424 | 3.12 ± 0.45 |
| | 30.0 ± 0.5 | | 293 | | 0.5 | 37.5 ± 1.0 | | 163 | |
| | 29.5 ± 1.0 | 3.0 ± 0.5 | 373 | 2.24 ± 0.54 | | 36.5 ± 1.0 | | 293 | |
| 0.78 | 33.4 ± 0.5 | 2.6 ± 0.6 | 112 | | | | $[\zeta\zeta 0]$ $T_2$ | | |
| | 32.2 ± 0.5 | | 293 | | | | | | |
| | 31.2 ± 0.5 | | 383 | | 0.079 | 5.7 ± 0.2 | 2.8 ± 0.1 | 110 | |
| 0.95 | 36.3 ± 0.5 | 2.9 ± 0.2 | 112 | | | 5.05 ± 0.25 | 2.2 ± 0.1 | 293 | 0.0 ± 0.14 |
| | 35.6 ± 0.5 | | 293 | | | 4.85 ± 0.25 | 2.4 ± 0.2 | 383 | 0.0 ± 0.22 |
| | | | | | | 4.85 ± 0.25 | 2.4 ± 0.1 | 424 | 0.0 ± 0.14 |
| | | | | | 0.316 | 19.1 ± 0.2 | 2.0 ± 0.1 | 110 | |
| | | | | | | 18.2 ± 0.2 | 2.9 ± 0.2 | 293 | 2.1 ± 0.22 |
| | | | | | | 17.8 ± 0.5 | 3.6 ± 0.4 | 383 | 2.99 ± 0.51 |
| | | | | | | 17.4 ± 0.5 | 3.9 ± 0.5 | 424 | 3.35 ± 0.51 |
| | | | | | 0.5 | 23.4 ± 0.3 | 2.6 ± 0.3 | 110 | |
| | | | | | | 22.15 ± 0.35 | 3.4 ± 0.4 | 293 | 2.20 ± 0.5 |
| | | | | | | 21.6 ± 0.5 | 3.8 ± 0.5 | 388 | 2.77 ± 0.64 |
| | | | | | | 21.0 ± 0.5 | 4.2 ± 0.5 | 424 | 3.30 ± 0.64 |
| | | $[\zeta\zeta\zeta]$ L | | | | | $[\zeta\zeta\zeta]$ T | | |
| 0.355 | 34.5 ± 0.5 | 3.6 ± 0.2 | 110 | | 0.129 | 9.0 ± 0.3 | 2.4 ± 0.4 | 110 | |
| | 33.3 ± 1.0 | 4.0 ± 0.6 | 297 | 1.74 ± 0.63 | | 8.4 ± 0.3 | | 293 | |
| | 33.0 ± 0.8 | 4.5 ± 0.6 | 395 | 2.7 ± 0.63 | 0.29 | 20.0 ± 0.5 | | 110 | |
| 0.516 | 29.5 ± 0.3 | | 110 | | | 18.3 ± 1.0 | | 293 | |
| | 27.2 ± 1.0 | | 393 | | 0.355 | 24.2 ± 0.5 | 3.6 ± 0.3 | 110 | |
| 0.677 | 16.4 ± 0.2 | 2.0 ± 0.1 | 110 | | | 22.5 ± 1.5 | 4.0 ± 0.5 | 293 | 1.74 ± 0.58 |
| | 15.1 ± 0.5 | 3.8 ± 0.2 | 296 | 3.23 ± 0.22 | | 22.0 ± 1.5 | | 395 | |
| | 13.8 ± 0.7 | 4.2 ± 0.5 | 394 | 3.69 ± 0.51 | 0.548 | 31.0 ± 0.5 | 3.2 ± 0.3 | 110 | |
| | 13.0 ± 0.5 | 4.2 ± 0.5 | 424 | 3.69 ± 0.51 | | 29.3 ± 1.0 | | 293 | |
| 0.839 | 28.0 ± 0.5 | 3.6 ± 0.5 | 110 | | 0.71 | 34.4 ± 0.8 | 3.4 ± 0.3 | 110 | |
| | 27.25 ± 1.0 | | 293 | | | 33.5 ± 1.0 | 4.0 ± 0.5 | 293 | 2.11 ± 0.58 |
| | | | | | 1.00 | 37.5 ± 1.0 | 3.5 ± 0.3 | 110 | |
| | | | | | | 35.8 ± 1.0 | 4.0 ± 0.5 | 293 | 1.94 ± 0.6 |
| | | | | | | 33.3 ± 1.0 | 4.8 ± 0.4 | 395 | 3.3 ± 0.5 |
| | | | | | | 33.1 ± 1.0 | 5.2 ± 0.5 | 424 | 3.85 ± 0.6 |

shown for the phonon at the $H$ point could be in error. The same could be true for the widths shown for the $[\zeta\zeta\zeta]$T branch.

## IV. CONCLUSION

Phonon dispersion relations in $^7$Li have been observed by coherent inelastic neutron scattering at 293 K. Some points for the $[\zeta\zeta\zeta]$T branch have also been measured at 110 K to complement the measurements by Smith *et al.*[1,7]

The phonon frequencies are significantly smaller at 293 K than at 110 K. The first-neighbor force constants at 293 K are about 10% lower than at low temperature.

The lattice parameter of $^7$Li has been measured at temperatures up to near the melting point and the observations are in good agreement with recent x-ray work up to 293 K. The value of the elastic

constants are (10–20)% higher than those from the sound-echo technique.

The temperature dependence of phonon energy shifts and linewidths for various $q$ values resemble qualitatively those obtained for potassium.[17] But the energy shifts are much larger in magnitude than those for potassium. Since lithium is the simplest metal it will be of great interest to perform the anharmonic calculations for comparison of the theory with the present experimental results.

ACKNOWLEDGMENTS

The authors would like to thank Dr. P. Platzman and Dr. J. Als-Nielsen for providing the $^7$Li metal. We must thank A. Thuesen and S. Jørgensen for their technical help during the crystal growing. One of the authors (M. M. B.) would like to thank the Danish Atomic Energy Commission for financial support during this work, and the Risø staff for their hospitality.

---

*Guest scientist from PINSTECH, P. O. Nilore, Rawalpindi, Pakistan.

[1]H. G. Smith, G. Dolling, R. M. Niclow, P. R. Vijayaraghavan, and M. K. Wilkinson, *Neutron Inelastic Scattering* (International Atomic Energy Agency, Vienna, 1968), Vol. I, p. 149.

[2]P. L. Srivastava and N. Mirshra, Phys. Lett. A 46, 219 (1973).

[3]A. D. B. Wood, B. N. Brockhouse, R. H. March, A. T. Stewart, and B. Bowers, Phys. Rev. 128, 1112 (1962).

[4]S. A. Werner and R. Pynn, J. Appl. Phys. 42, 4736 (1971).

[5]J. E. D. Copley, B. N. Brockhouse, and S. H. Cohen, in Ref. 1, p. 209.

[6]E. R. Cowley and A. K. Pant, Acta Crystallgr. A 26, 439 (1970).

[7]H. G. Smith, G. Dolling, R. M. Nicklow, P. R. Vijayaraghavan, and M. K. Wilkinson, ORNL-4408, UC-34, Physics, 1969 (unpublished).

[8]M. M. Beg, Risø Report No. M-1791, 1974 (unpublished).

[9]G. Raunio, L. Almquist, and R. Stedman, Phys. Rev. 178, 1496 (1969).

[10]G. Gilat and L. J. Raubenheimer, Phys. Rev. 144, 390 (1966).

[11]D. L. Martin, Physica 25, 1193 (1959).

[12]T. H. K. Barron, in *Lattice Dynamics*, edited by R. F. Wallis (Pergamon, New York, 1965), p. 247.

[13]M. R. Nadler and C. P. Kempter, Anal. Chem. 31, 2109 (1959).

[14]V. S. Kogan and V. I. Khotkevic, Zh. Eksp. Teor. Fiz. 42, 916 (1962) [Sov. Phys.-JETP 15, 632 (1962)].

[15]H. C. Nash and C. S. Smith, J. Phys. Chem. Solids 9, 113 (1959).

[16]A. L. Jain, Phys. Rev. 123, 1234 (1961).

[17]W. J. L. Buyers and R. A. Cowley, Phys. Rev. 180, 755 (1969).